

Supporting Information

Coupling of Cerium Oxide Cyanamide with Fe-N-C for Enhanced Oxygen Reduction Reaction

Xu Zhang^{abc}, Jingxian Zhang^{bc}, Shi Zeng^{bc} Haifan Wang^{bc}, Yiling Bai^{de}, Huaming Hou^{de}, Ke Zhang^f, Bin Li^{f*}, and Guangjin Zhang^{bc*}

^a College of Chemical Engineering, Shenyang University of Chemical Technology, Shenyang 110142, China

^b Center of Materials Science and Optoelectronics Engineering, University of Chinese Academy of Sciences, Beijing 100049, China

^c CAS Key Laboratory of Green Process and Engineering, Institute of Process Engineering, Chinese Academy of Sciences, 100190, Beijing, China

^d State Key Laboratory of Coal Conversion, Institute of Coal Chemistry, Chinese Academy of Sciences, Taiyuan 030001, China

^e National Energy Center for Coal to Liquids, Synfuels China Technology Co., Ltd, Beijing 101400, PR China

^f Zhengzhou Tobacco Research Institute of CNTC, Zhengzhou 450001, China

Supporting Figures and Tables

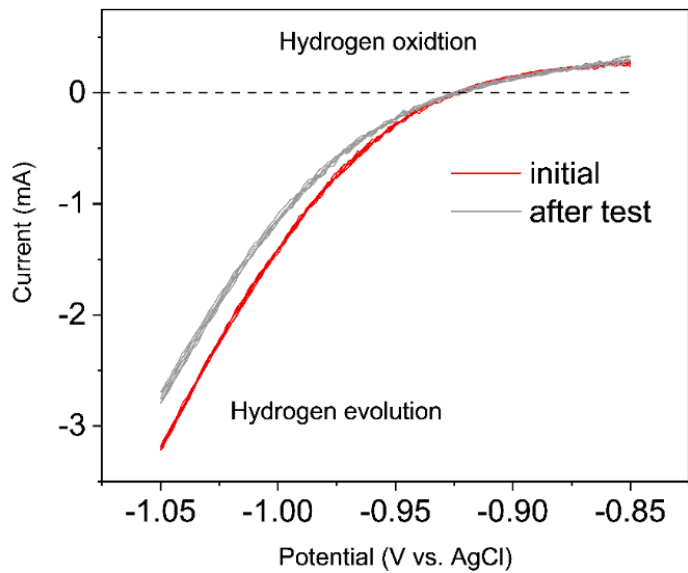


Fig. S1. Reversible hydrogen electrode (RHE) calibration results in 0.1 M KOH solution at a scan rate of 1 mV s⁻¹.

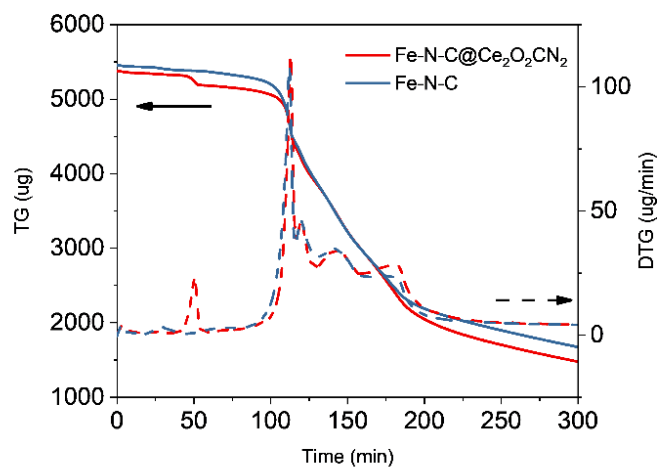


Fig. S2. TG analysis of the Fe-ZIF-8@Ce₂O₂CN₂ and Fe-ZIF-8.

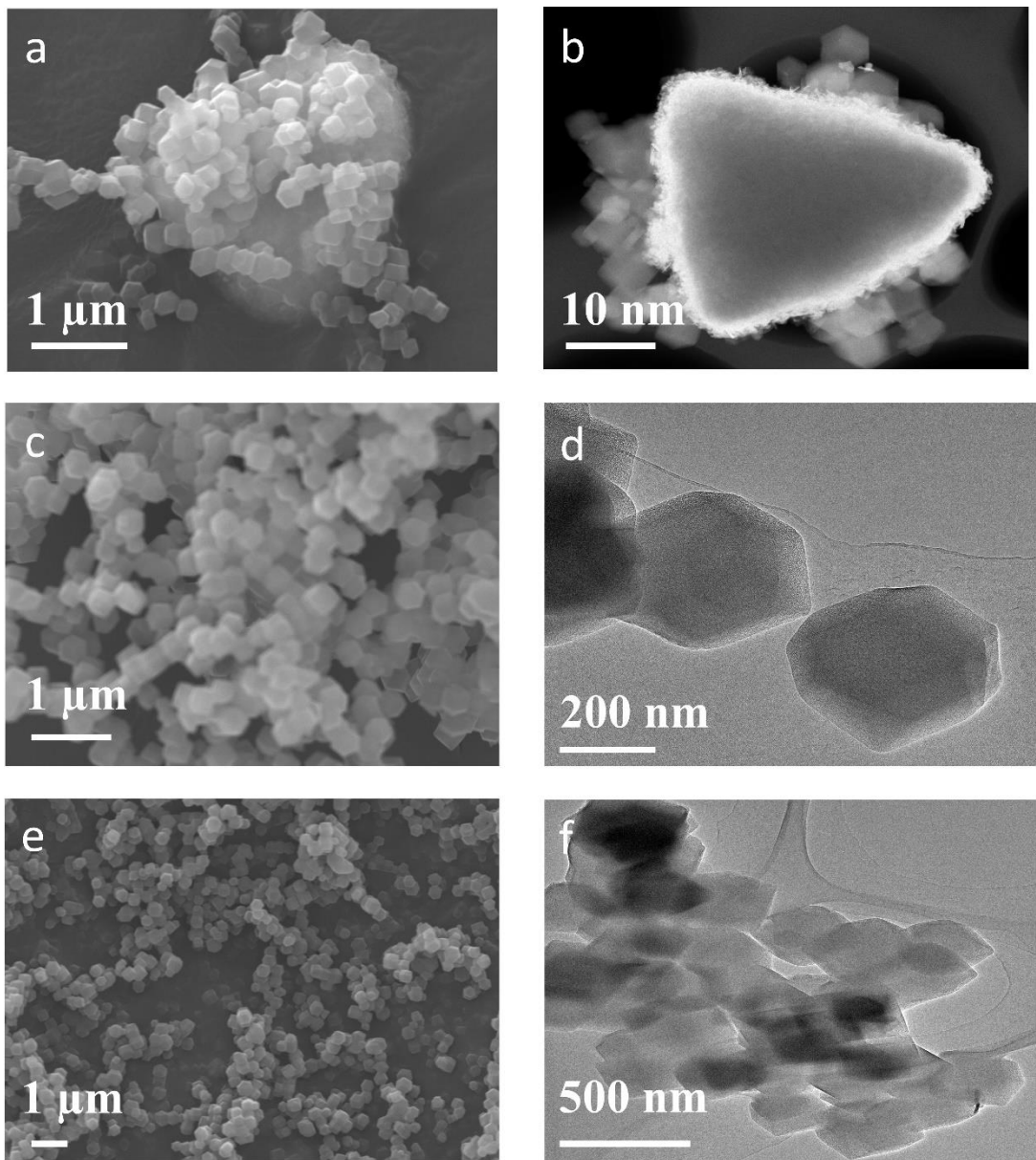


Fig. S3. SEM and TEM images of (a,b) N-C@Ce₂O₂CN₂, (c,d) Fe-N-C, and (e,f) N-C.

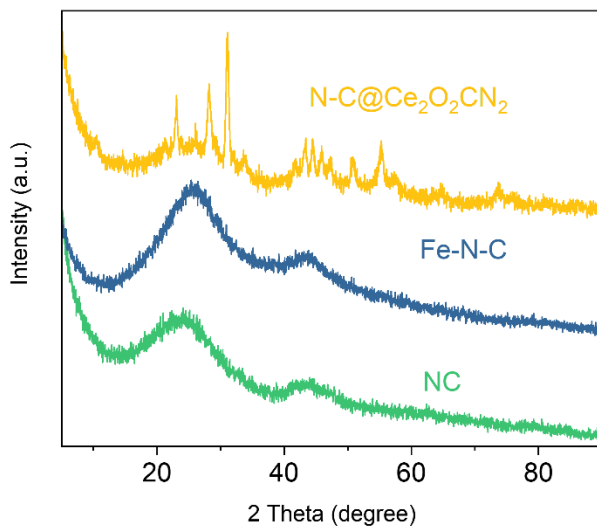


Fig. S4. PXRD patterns of N-C@Ce₂O₂CN₂, Fe-N-C, and NC.

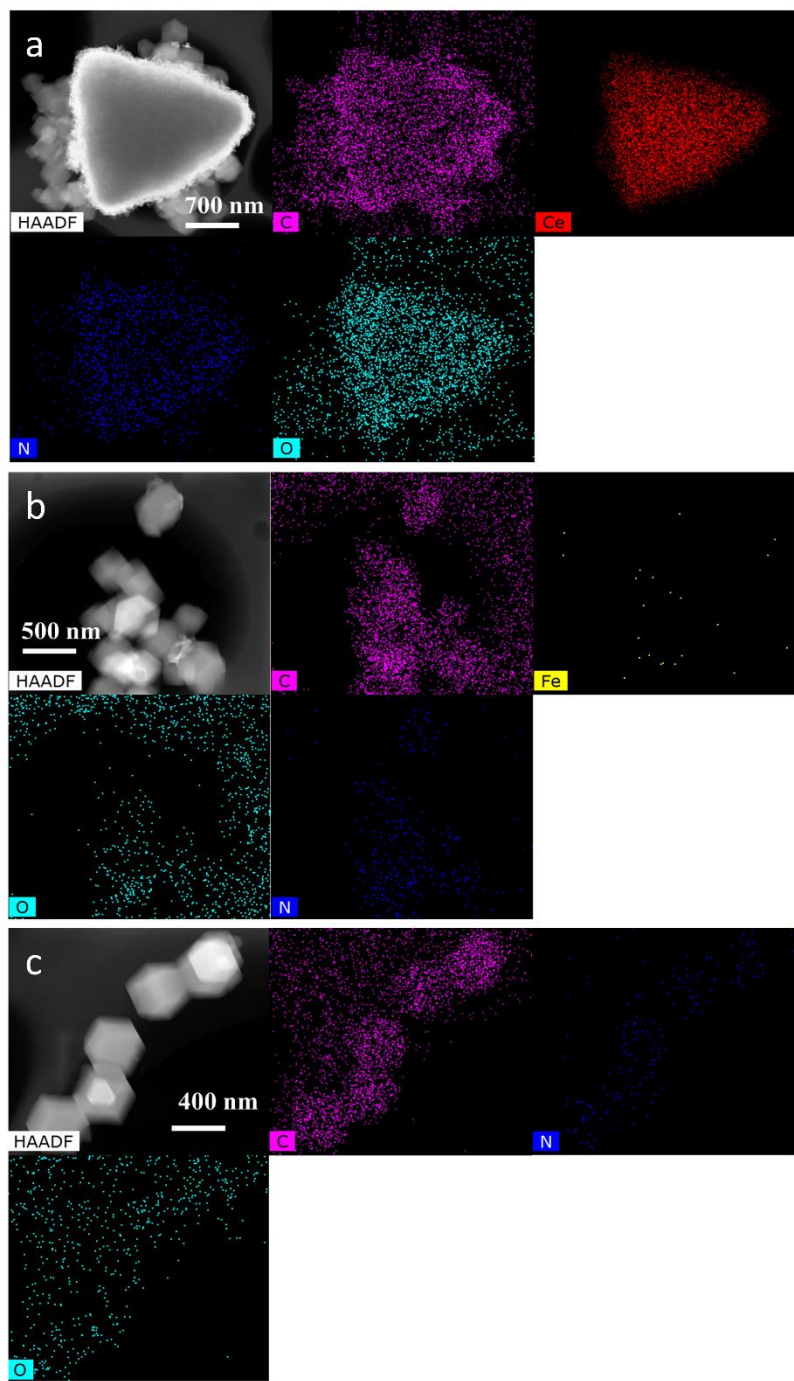


Fig. S5. HADDF-STEM images and corresponding EDS elemental mappings of (a) N-C@Ce₂O₂CN₂, (b) Fe-N-C, and (c) N-C.

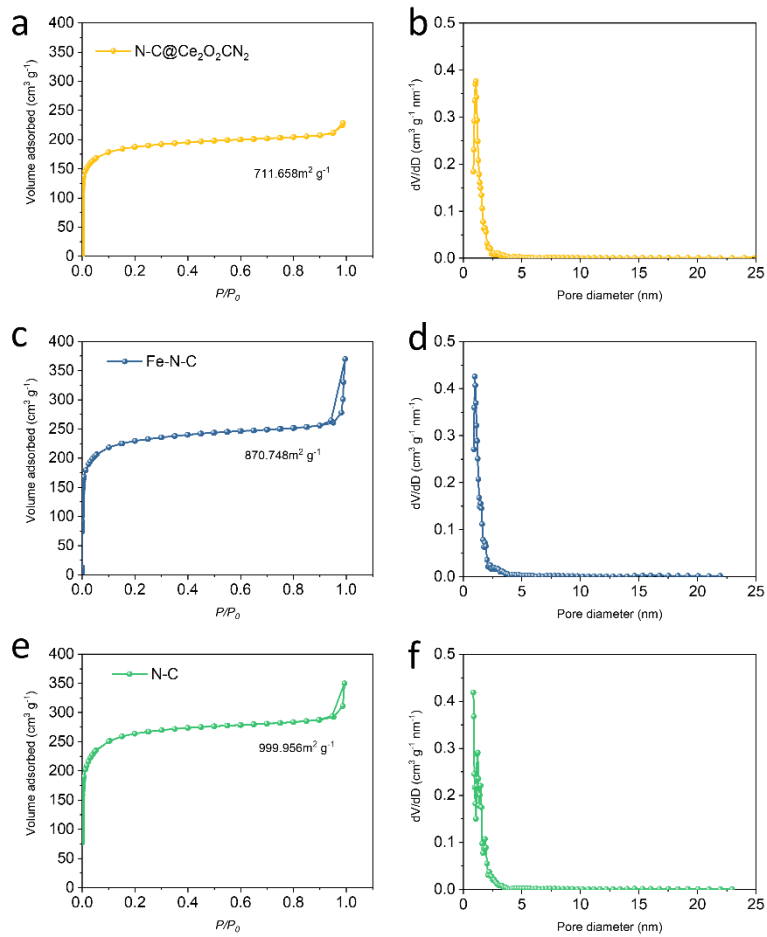


Fig. S6. N₂ adsorption-desorption isotherms and pore size distributions of (a,b) N-C@Ce₂O₂CN₂, (c,d) Fe-N-C, and (e,f) N-C.

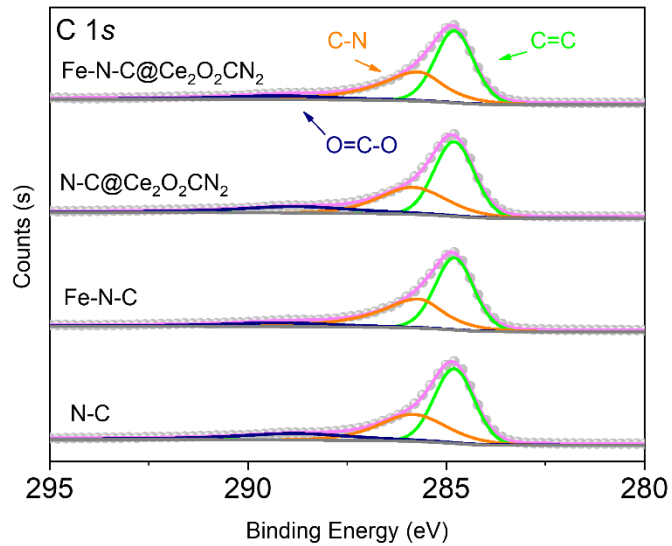


Fig. S7. High resolution XPS spectra for C 1s in all samples.

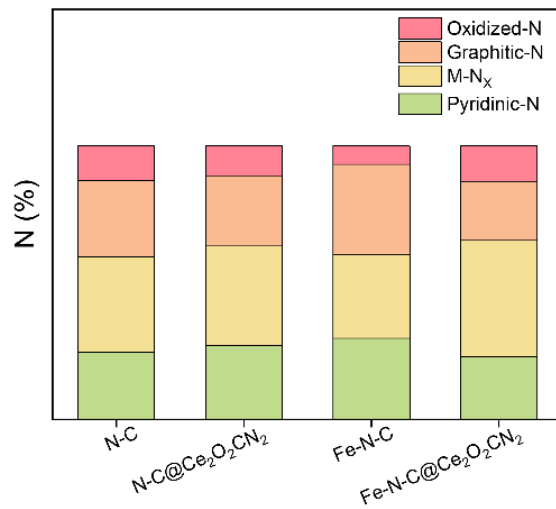


Fig. S8. The atomic percentage of pyridinic-N, M-N_x, graphitic-N, and oxidized-N of obtained catalysts.

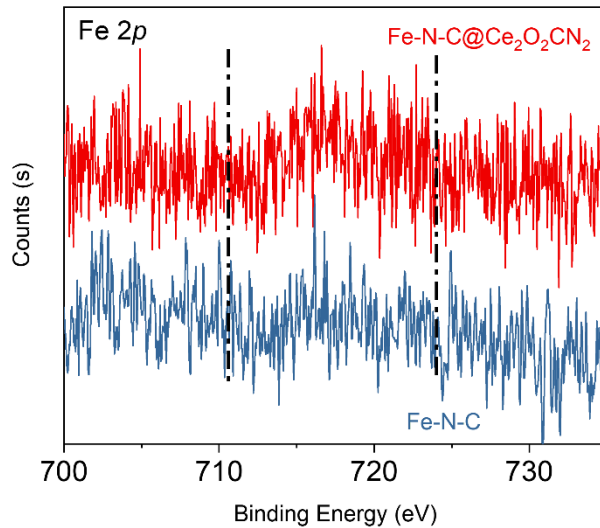


Fig. S9. High resolution XPS spectra for Fe 2p in Fe-N-C@Ce₂O₂CN₂ and Fe-N-C.

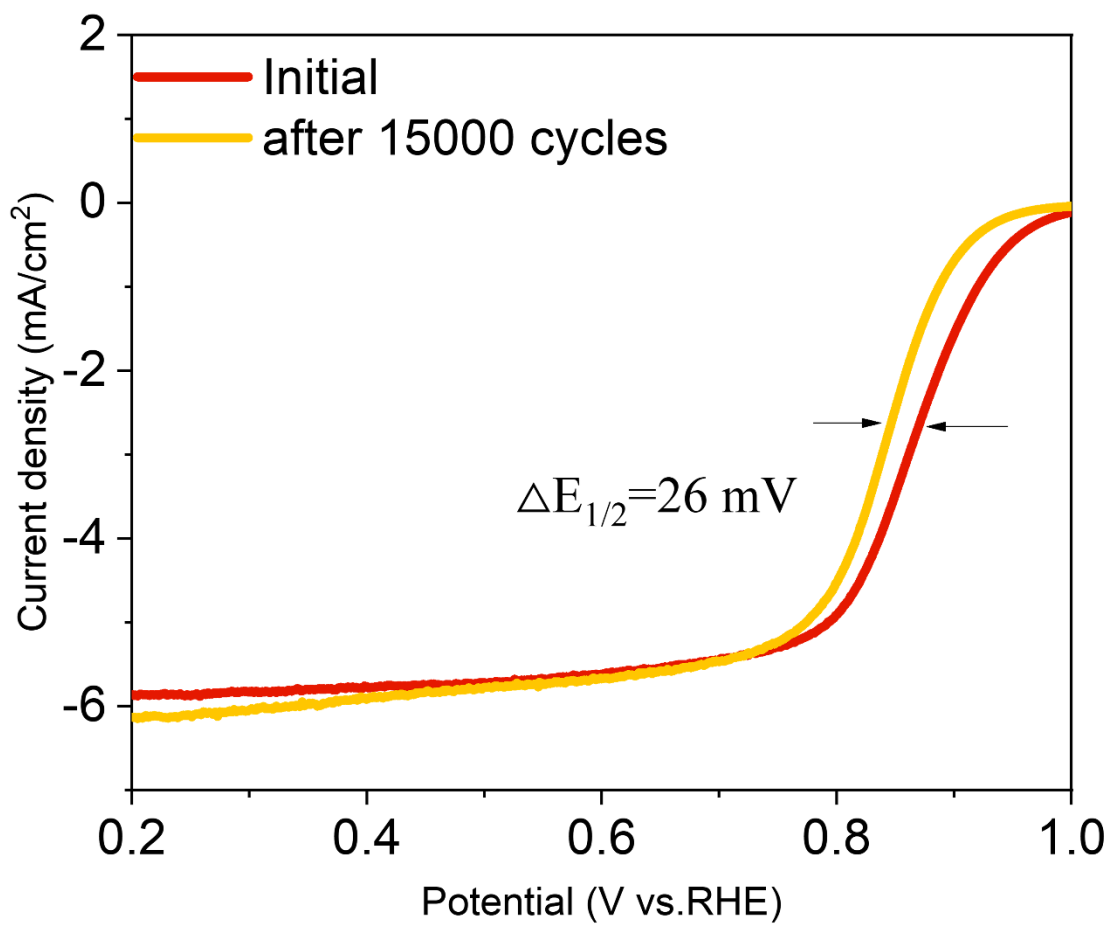


Fig. S10. RDE polarization curves of Pt/C before and after 15000 cycles ranging from 0.6 to 1.1 V at 500 mV/s in O_2 -saturated 0.1 M KOH.

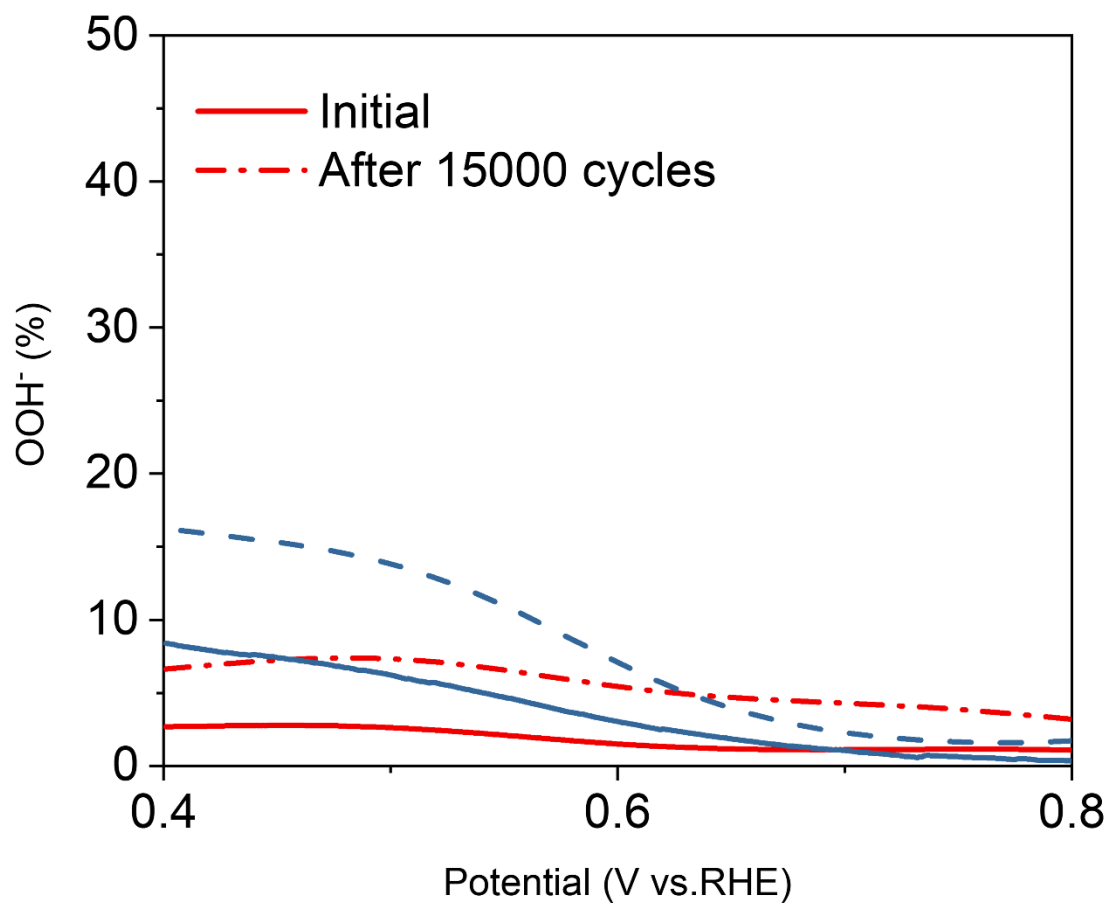


Fig. S11. OOH⁻ yields of Fe-N-C@Ce₂O₂CN₂ (red) and Fe-N-C (blue) before and after 15000 cycles accelerated durability tests.

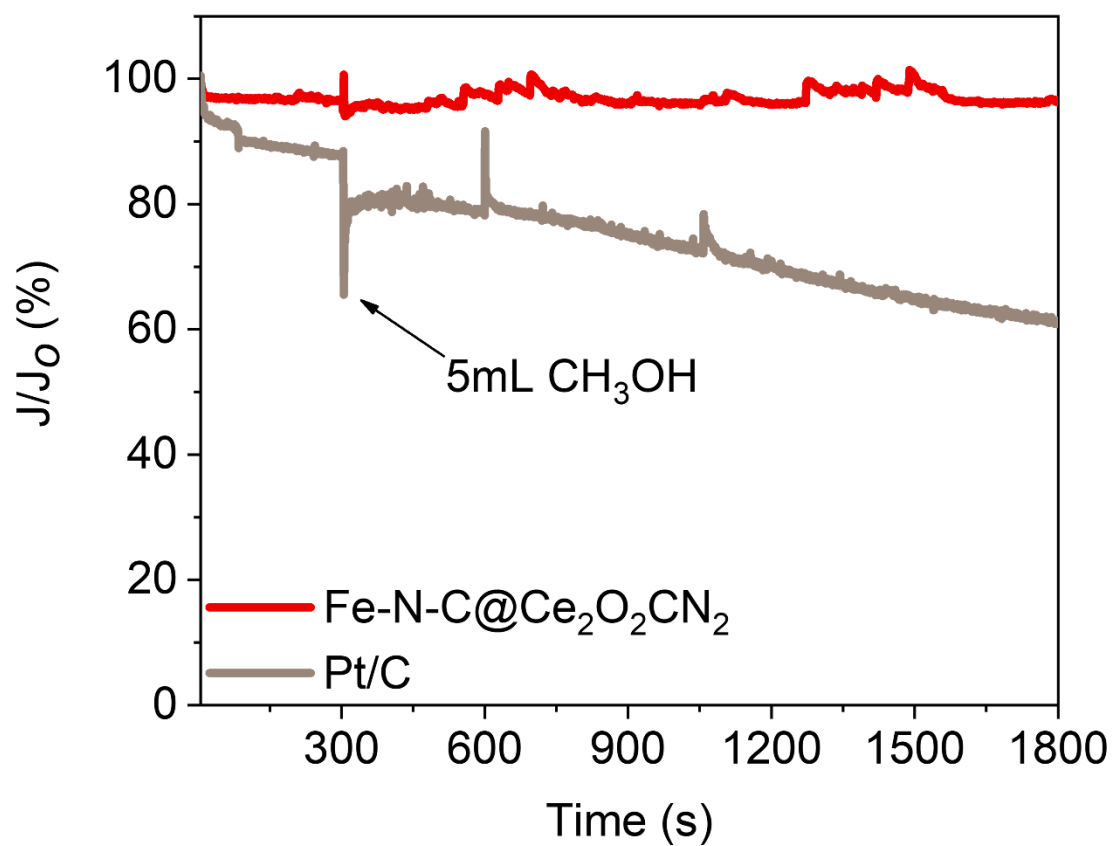


Fig. S12. Chronoamperometric responses of Pt/C at 0.5 V after injecting 5 ml methanol into 180 ml 0.1 M KOH.

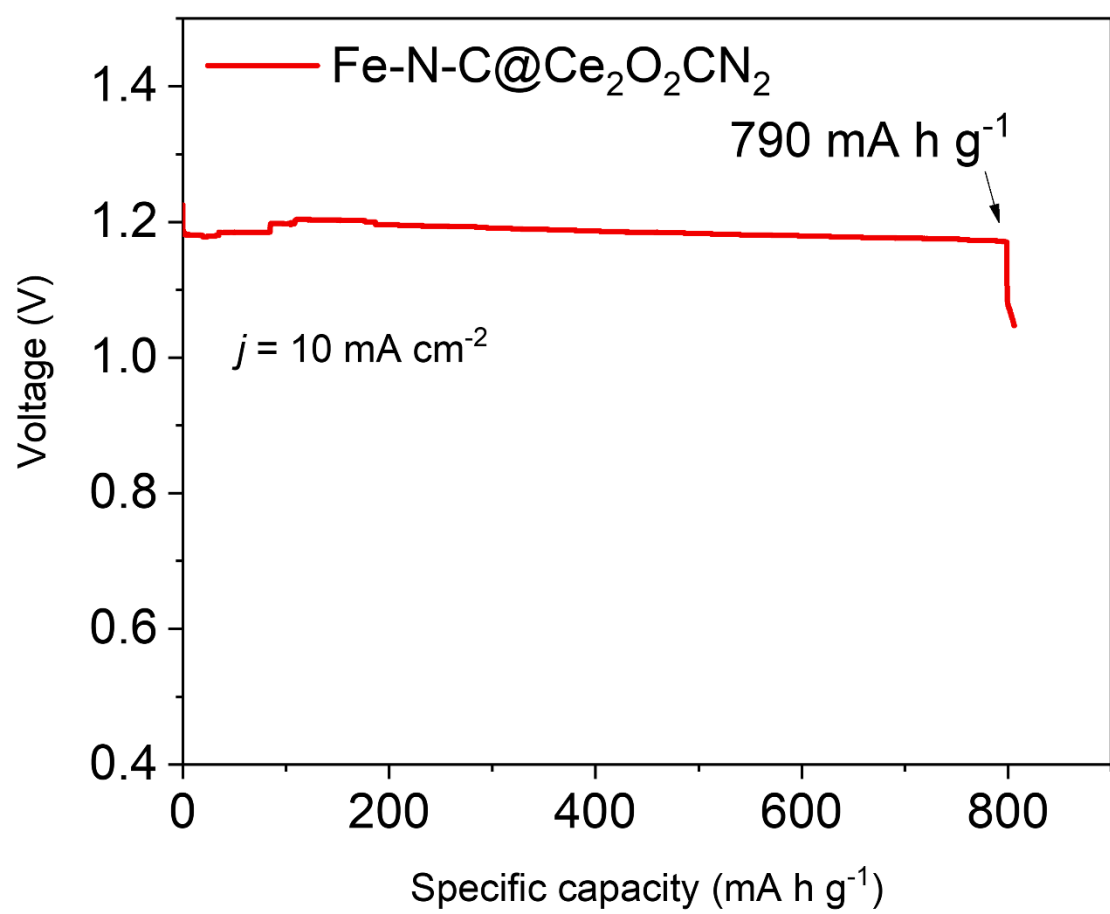


Fig. S13. Specific capacity of Fe-N-C@ $\text{Ce}_2\text{O}_2\text{CN}_2$.

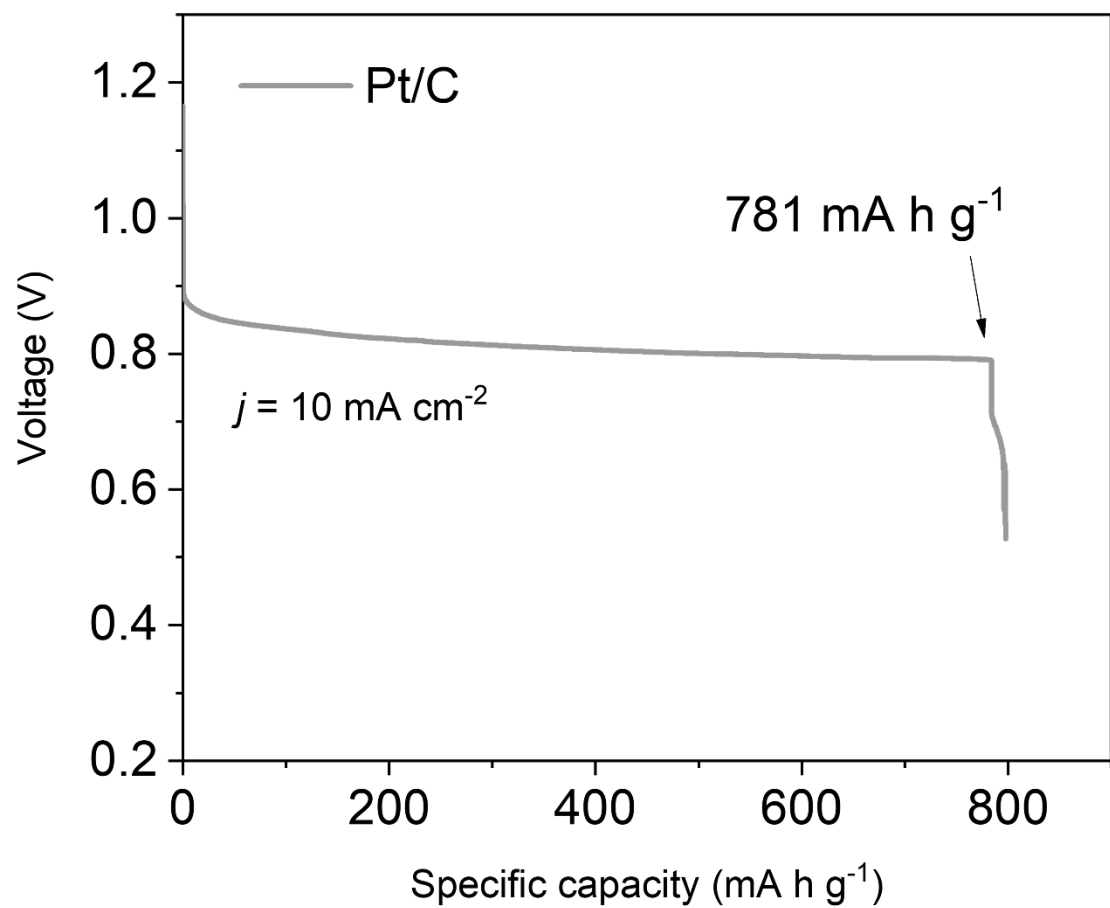


Fig. S14. Specific capacity of Pt/C.

Table S1. Comparison of ORR electrocatalysis performance of the as-prepared catalyst with reported catalysts.

Samples	E _{ONSET} (V vs. RHE)	E _{1/2} (V vs. RHE)	Reference
Fe-N-C@Ce ₂ O ₂ CN ₂	0.951	0.89	This work
Fe-N-C-2HT-1AL	0.92	0.82	¹
Fe-N-CC	0.94	0.83	²
p-Fe-N-CNFs	0.91	0.82	³
Fe-NC SAC	0.98	0.90	⁴
Fe-N/P-C-700	0.941	0.867	⁵
Fe2-Z8-C	0.985	0.871	⁶
CNT@f-FeNC170	0.97	0.84	⁷
Fe-N-C/MXene	0.92	0.84	⁸

Table S2. Comparison of ZABs performance of the as-prepared catalyst with reported catalysts.

Samples	OCP (V)	P _{max} (mV/cm ²)	Reference
Fe-N-C@Ce ₂ O ₂ CN ₂	1.43	120	This work
FeCo NPs–N–CNTs	1.51	116	⁹
CoN4/NG	1.51	115	¹⁰
Co ₃ FeS _{1.5} (OH) ₆	-	113.1	¹¹
Fe-N/C-1/30	1.525	121.8	¹²
CoNi-SAs/NC	1.45	101.4	¹³
Pd/FeCo	1.42	117	¹⁴
FeCoMoS@NG	1.44	118	¹⁵
Fe-2-WNPC-NCNTs	1.43	101.3	¹⁶

References

1. N. R. Sahraie, U. I. Kramm, J. Steinberg, Y. Zhang, A. Thomas, T. Reier, J.-P. Paraknowitsch and P. Strasser, *Nature Communications*, 2015, **6**, 8618.
2. G. A. Ferrero, K. Preuss, A. Marinovic, A. B. Jorge, N. Mansor, D. J. L. Brett, A. B. Fuertes, M. Sevilla and M.-M. Titirici, *ACS Nano*, 2016, **10**, 5922-5932.
3. B.-C. Hu, Z.-Y. Wu, S.-Q. Chu, H.-W. Zhu, H.-W. Liang, J. Zhang and S.-H. Yu, *Energy & Environmental Science*, 2018, **11**, 2208-2215.
4. L. Zhao, Y. Zhang, L.-B. Huang, X.-Z. Liu, Q.-H. Zhang, C. He, Z.-Y. Wu, L.-J. Zhang, J. Wu, W. Yang, L. Gu, J.-S. Hu and L.-J. Wan, *Nature Communications*, 2019, **10**, 1278.
5. K. Yuan, D. Lützenkirchen-Hecht, L. Li, L. Shuai, Y. Li, R. Cao, M. Qiu, X. Zhuang, M. K. H. Leung, Y. Chen and U. Scherf, *Journal of the American Chemical Society*, 2020, **142**, 2404-2412.
6. Q. Liu, X. Liu, L. Zheng and J. Shui, *Angewandte Chemie International Edition*, 2018, **57**, 1204-1208.
7. G. Zhang, Y. Jia, C. Zhang, X. Xiong, K. Sun, R. Chen, W. Chen, Y. Kuang, L. Zheng, H. Tang, W. Liu, J. Liu, X. Sun, W.-F. Lin and H. Dai, *Energy & Environmental Science*, 2019, **12**, 1317-1325.
8. L. L. Jiang, J. J. Duan, J. W. Zhu, S. Chen and M. Antonietti, *Acs Nano*, 2020, **14**, 2436-2444.
9. T. Zhang, J. Bian, Y. Zhu and C. Sun, *Small*, 2021, **17**, 2103737.
10. L. Yang, L. Shi, D. Wang, Y. Lv and D. Cao, *Nano Energy*, 2018, **50**, 691-698.
11. H.-F. Wang, C. Tang, B. Wang, B.-Q. Li and Q. Zhang, *Advanced Materials*, 2017, **29**, 1702327.
12. W. Wei, X. Shi, P. Gao, S. Wang, W. Hu, X. Zhao, Y. Ni, X. Xu, Y. Xu, W. Yan, H. Ji and M. Cao, *Nano Energy*, 2018, **52**, 29-37.
13. X. Han, X. Ling, D. Yu, D. Xie, L. Li, S. Peng, C. Zhong, N. Zhao, Y. Deng and W. Hu, *Advanced Materials*, 2019, **31**, 1905622.
14. F. Pan, Z. Li, Z. Yang, Q. Ma, M. Wang, H. Wang, M. Olszta, G. Wang, Z. Feng, Y. Du and Y. Yang, *Advanced Energy Materials*, 2021, **11**, 2002204.
15. S. Ramakrishnan, J. Balamurugan, M. Vinothkannan, A. R. Kim, S. Sengodan and D. J. Yoo, *Applied Catalysis B: Environmental*, 2020, **279**, 119381.
16. Z. Liu, Y. Zhu, K. Xiao, Y. Xu, Y. Peng, J. Liu and X. Chen, *ACS Applied Materials & Interfaces*, 2021, **13**, 24710-24722.